Atmos. Chem. Phys. Discuss., 10, 9219–9252, 2010
www.atmos-chem-phys-discuss.net/10/9219/2010/


Atmospheric Chemistry and Physics Discussions

This discussion paper is/has been under review for the journal Atmospheric Chemistry and Physics (ACP). Please refer to the corresponding final paper in ACP if available.

# Updraft and downdraft characterization with Doppler lidar: cloud-free versus cumuli-topped mixed-layer

**A. Ansmann, J. Fruntke, and R. Engelmann**

Leibniz Institute for Tropospheric Research, Permoserstr. 15, 04318 Leipzig, Germany

Received: 12 March 2010 – Accepted: 4 April 2010 – Published: 13 April 2010

Correspondence to: A. Ansmann (albert@tropos.de)

Published by Copernicus Publications on behalf of the European Geosciences Union.





## Abstract

For the first time, a comprehensive, height-resolved Doppler lidar study of updrafts and downdrafts in the mixing layer is presented. The Doppler lidar measurements were performed at Leipzig, Germany, in the summer half year of 2006. The conditional sampling method is applied to the measured vertical velocities to identify, count, and analyze significant updraft and downdraft events. Three cases of boundary layer evolution with and without fair weather cumuli formation are discussed. Updrafts occur with an average frequency of 1–2 per unit length $z_i$ (boundary layer depth $z_i$), downdrafts 20%–30% more frequently. In the case with cumuli formation, the draft occurrence frequency is enhanced by about 50% at cloud level or near cloud base. The counted updraft events cover 30%–34%, downdrafts 53%–57% of the velocity time series during the main period of convective activity. By considering all drafts with horizontal extent >36 m in the analysis, the updraft mean horizontal extent ranges from 200–350 m and is about $0.15z_i$ in all three cases. Downdrafts are a factor of 1.3–1.5 larger. The average value of the updraft mean vertical velocities is 0.5–0.7 m/s or $0.4w_*$ (convective velocity scale $w_*$), and the negative downdraft mean vertical velocities are weaker by roughly 10%–20%. The analysis of the relationship between the size (horizontal extent) of the updrafts and downdrafts and their mean vertical velocity reveals a pronounced increase of the average vertical velocity in updrafts from 0.4–0.5 m/s for small thermals (100–200 m) to about 1.5 m/s for large updrafts (>600 m) in the case with fair weather cumuli. At cloudless conditions, the updraft velocities were found to be 20% smaller for the large thermals.

## 1 Introduction

It is well known that vertical mixing of heat, moisture, momentum, aerosols, and gaseous pollution in the unstable atmospheric boundary layer (ABL) is predominantly carried out by motions occurring within discrete elements of considerable vertical extent



ACPD

10, 9219–9252, 2010



(Lenschow, 1970; Lenschow and Stephens, 1980; Greenhut and Khalsa, 1982, 1987; Khalsa and Greenhut, 1985; Young, 1988a,b,c). Convectively driven updrafts formed by coalescence of smaller surface-based buoyant elements often extend through the depth of the well-mixed layer. Coherent thermals up to 4 km height above ground are found over desert areas (Ansmann et al., 2009). Thermals of sufficient size and buoyancy reaching the capping inversion penetrate into the stable layer above and cause dry air intrusions which sometimes reach heights close to the surface in form of well-organized downdrafts. These upward and the compensating downward motions are responsible for an efficient vertical exchange in the ABL. Therefore, field observations of the number frequency of occurring updrafts and surrounding downdraft areas, their typical horizontal extents and strengths in terms of updraft and downdraft mean vertical velocities provide valuable information to improve our understanding of the physical processes of organized convection in the ABL and to further improve and validate vertical flux schemes of atmospheric models.

Boundary layer clouds such as fair weather cumuli (cumulus humilis, mediocris, congestus) have a significant impact on the vertical transport characteristics (Young, 1988c; Kollias et al., 2001). The interaction between boundary layer cumulus clouds and thermals which initiate them is of considerable importance not only to the turbulence structure of the convective boundary layer but also to the venting of pollutants into the free atmosphere and the triggering of deep moist convection (Young, 1988c). Active cumulus (e.g., cumulus congestus) with an additional energy source due to the release of latent heat enhances mixed layer turbulence and can thus significantly alter the updraft profile. Representing these processes realistically in atmospheric models including the development of appropriate cloud parameterizations continues to be a challenging task.

To better understand this complex field of atmospheric physics, more updraft/downdraft field observations are required. Studies under very different meteorological conditions, for different weather regimes, at maritime and continental sites, in rural and urban environments, over flat and orographically complex terrain are useful.





More than 20 years after the pioneering work by Lenschow, Greenhut, Khalsa, and Young, a first comprehensive lidar-based study of updraft and downdraft occurrence frequencies, occurrence durations, corresponding horizontal extents, and mean vertical velocities of updrafts and downdrafts is presented. In contrast to airborne in situ observations (Lenschow and Stephens, 1980; Greenhut and Khalsa, 1982; Khalsa and Greenhut, 1985; Godowitch, 1986; Young, 1988b; Williams and Hacker, 1992; Durand et al., 2000; Said et al., 2010), Doppler lidar allows us to monitor the entire mixed layer including the entrainment zone vertically resolved and continuously over long time periods so that a detailed study of the full evolution cycle of the ABL over the day is possible (Grund et al., 2001; Bösenberg and Linné, 2002; Drobinski et al., 2004; Wulfmeyer and Janjić, 2005; Lothon et al., 1986; Gibert et al., 2007; Engelmann et al., 2008; Hogan et al., 2009).

During the Aerosol Vertical ExChange 2006 (AVEC 2006) campaign from March to November 2006, we observed more than 70 diurnal cycles of the ABL evolution with a zenith-pointing Doppler lidar in flat terrain at a central European urban site (Leipzig, Germany). The Doppler lidar measures height profiles of the vertical wind component with a temporal and vertical resolution of 5 s and 75 m. In this paper we study the ABL updraft and downdraft characteristics of three cases following the strategy suggested by Young (1988b). The frequency of occurrence of updrafts and downdrafts, their occurrence duration and corresponding horizontal extent, the vertical velocities in the drafts as well as the relationship between the draft mean velocity and draft horizontal size are investigated. We extend the traditional discussion by contrasting the findings for a cloud-free case and a case with fair weather cumuli formation. The selected three cases can be regarded as representative for many summertime ABL developments over Leipzig.

In Sect. 2, the AVEC campaign, the Doppler lidar, and the data analysis method are explained. Section 3 presents the results of the three case studies of PBL evolution. A summary and concluding remarks are given in Sect. 4.





## 2 Experiment

In the framework of AVEC 2006, for the first time well-coordinated observations of the vertical flux of atmospheric aerosol particles were performed by utilizing a wind Doppler lidar in synchronized combination with a multiwavelength aerosol Raman lidar (Engelmann et al., 2008). AVEC 2006 took place at Leipzig (51.4° N, 12.4° E, 120 m above sea level, rather flat terrain) from 1 March to 31 October 2006. As part of AVEC 2006, Baars et al. (2008) analyzed one-year observations of the ABL evolution with a quasi continuously running automated aerosol lidar and present statistics on the daytime ABL top height $z_i$ and $z_i$ growth rates during the morning hours. The third goal of AVEC 2006 is the detailed characterization of ABL turbulent motions in terms of updraft and downdraft properties.

The utilized Doppler lidar measures the vertical velocity of aerosol particles and thus of air parcels from 400 m above the ground to the top of the ABL with 5 s temporal and 75 m vertical resolution as mentioned. The Doppler lidar is described in detail by Engelmann et al. (2008) and Engelmann (2009). The transmitted wavelength is 2.022 µm. The zero wind speed is checked from time to time by pointing the laser beam to a building. The remaining uncertainty after this calibration is estimated to be 0.05 m/s. The overall uncertainty in the determination of the vertical velocity is of the order of 0.10–0.15 m/s, taking an uncertainty of 0.05 m/s in the signal processing and a similar uncertainty resulting from the pointing uncertainty of 0.2° into account. The vertical alignment was often checked by rocking over the zenith from −2° to +2° and searching for the peak in the backscatter signal caused by specular reflections when cirrus is present (Seifert et al., 2008).

The basic data analysis (noise filtering, signal digitization, fast Fourier transformation, spectral peak finding) to determine the wind speed is presented by Engelmann (2009) and Fruntke (2009). From the wind data set we removed outliers, i.e., unrealistic clear air vertical wind values of >10 m/s and < −10 m/s and wind speed values that differed significantly from neighboring values.



ACPD
10, 9219–9252, 2010



We applied the conditional sampling technique (Greenhut and Khalsa, 1982, 1987; Young, 1988b) to the remaining data set to identify the updraft and downdraft regions and to estimate their horizontal and vertical extent. We count a data sequence as updraft or downdraft event when the condition

$$w(t) > 0.1 \text{ m/s} \quad (1)$$

or

$$w(t) < -0.1 \text{ m/s} \quad (2)$$

is fulfilled for $t \geq 20$ s. $w$ is the vertical velocity. We assume $\overline{w} = 0$ and check this assumption by averaging wind velocities in the early morning hours before the evolution of the PBL or late evening hours after the formation of the residual layer. The threshold value of $w = 0.1$ m/s allows us to concentrate on the significant updrafts and downdrafts. The choice of a $w$ threshold and a minimum width controls the differentiation of thermals from regions of mesoscale ascents (of a few cm/s) and from small-scale fluctuations on thermals (Young, 1988b). Those remaining data points in the time series that satisfy neither the criteria for thermal updraft nor between-thermal downdraft are grouped into a third category called environmental air (Stull, 1988).

By flying cross and parallel to the main wind directions, Williams and Hacker (1992) showed that the horizontal cross sections of updraft and downdraft zones depend on flight leg (perpendicular or parallel to the wind direction) in the surface layer (at heights $< 0.1 z_i$) but not in the mixing layer ($> 0.3 z_i$), so that ground-based lidar observations (parallel to the main wind direction) in the mixing layer provide a trustworthy view into the updraft and downward characteristics.

Among the set of quantities characterizing the turbulent state of the boundary layer, the vertical velocity variance $\sigma_w^2$, skewness $s_w$, and kurtosis $k_w$ defined as

$$\sigma_w^2(z) = \overline{w(z)^2}, \quad (3)$$

$$s_w(z) = \overline{\left(\frac{w(z)}{\sigma_w(z)}\right)^3} \quad (4)$$





$$k_w(z) = \overline{\left(\frac{w(z)}{\sigma_w(z)}\right)^4} - 3. \quad (5)$$

are used. Note that $s_w = 0$ and $k_w = 0$ for an ideal Gaussian distribution according to Eq. (5).

An important quantity in the description of convective motions is the convective velocity scale $w_*$. The vertical velocity scale is estimated by applying the relationship (Lenschow and Stephens, 1982)

$$\sigma_w^2(z) = 1.8 w_*^2 \left(\frac{z}{z_i}\right)^{\frac{2}{3}} \left(1 - 0.8\frac{z}{z_i}\right)^2. \quad (6)$$

with height $z$ and the mixing layer depth $z_i$. The measured profile of $\sigma_w^2(z)$ is compared to respective $\sigma_w^2(z)$ profiles computed after Eq. (6) for a large set of $z_i$ and $w_*$ pairs. The most appropriate curve and respective values for $z_i$ and $w_*$ are found by fitting (least squares fit) the modelled curve (Eq. 6) to the measured profile of $\sigma_w^2(z)$ (Eq. 3). The analysis is facilitated if the mixing-layer depth $z_i$ is known from a simultaneously running aerosol lidar or ceilometer so that only $w_*$ remains to be determined. As outlined in Stull (1988) the whole process of vertical mixing is a circulation that moves air up and down in the mixed layer with a time period on the order of $t_* = z_i/w_*$ in the case of surface-heating-driven convection. For $z_i = 1000$ m and $w_* = 1$ m/s, we obtain $t_* = 1000$ s, i.e., about 15 min are needed for one full circle.

## 3 Results

### 3.1 Meteorological and turbulence characteristics

Figure 1 shows the three selected cases. On 5 May 2006, a 2–2.5 km deep, cloud-free ABL developed. A high pressure system over Scandinavia and a low pressure

system over southeastern Europe caused advection of dry eastern European air to the lidar field site. Easterly winds with velocities around 10 m/s prevailed in the mixing layer (above 500 m) up to the boundary layer top $z_i$ as indicated by nearby radiosonde profiles and atmospheric modeling results (data archive of the US National Weather Service's National Center of Environmental Prediction based on the Global Data Analysis System, http://www.arl.noaa.gov/fnl.php).

On 18 September 2006 (see Fig. 1, center panel), the air mass was advected from southerly to westerly directions under the influence of a weak, dissolving low pressure system over eastern Germany. Wind speeds were low with values of $< 2$ m/s. An optically thin lofted Saharan dust layer from 2–4 km height may have influenced (dampened) the ABL development before 13:00 Local Time (LT, 11:00 UTC, 12:00 Central European Time).

The 5 April case shown in the bottom panel of Fig. 1 represents a typical case of an ABL evolution with fair weather cumuli formation. Under the influence of a low pressure system over the Baltic Sea (Denmark, southern Sweden) cold and dry air of polar origin was advected from the North Sea to the field site on that day. Northwesterly winds were weak with wind speeds $< 5$ m/s. Fair weather cumulus clouds developed one hour after the onset of the ABL evolution. The cloud base height increased from 500 to 1500 m during the day. According to a simultaneously operated small aerosol lidar, the boundary-layer top height increased from 1075 to 1700 m (5 April), 1900 to 2350 m (5 May), and from 450 to 1450 m (18 September) within the time period from 12:00 to 16:00 LT.

Figure 2 presents profiles for the statistical moments (variance, skewness, and kurtosis) computed after Eqs. (3–5) for two-hour intervals during phases of strong convection. The vertical velocity variance decreases with height, i.e., with distance from the source of turbulent kinetic energy (TKE) production. $\sigma_w^2$ is highest on 5 May, the day with the deepest ABL and the highest $w_*$.

Skewness is positive which indicates surface-heating-driven convection and that, in a very idealized sense, broad regions of gentle downdraft surround smaller regions

of strong updraft (Moeng and Rotunno, 1990; Hogan et al., 2009). The skewness is highest for the day with fair-weather cumuli development (5 April) and lowest at the cloud-free day (5 May).

A measure of the peakedness of a distribution is the normalized fourth moment or kurtosis. Positive kurtosis indicates that the distribution of vertical velocity fluctuations in the mixing layer is much more peaked than a Gaussian distribution. The highest kurtosis values are found on the day with fair weather cumuli.

Figure 3 shows histograms of vertical velocities for 525 and 970 m height measured on 5 April 2006 from 09:49–16:45 LT (almost for the entire measurement period in Fig. 1). Measurements after 16:45 LT, when a compact almost closed stratocumulus field was present over the field site above 1500 m height, are not considered. Both distributions in Fig. 3 are shifted to the left. This shift is caused by the occurrence of a large number of weak interthermal downdrafts, and a small frequency of strong thermal updrafts (Stull, 1988). The skewness (positive after Eq. (4) in this case) decreases with height. The velocity distribution tend to become more symmetric.

### 3.2 Updraft and downdraft statistics

Figure 4 presents an idealized and simple sketch in order to illustrate what a Doppler lidar is detecting. In the case of easterly winds, the lidar is monitoring the ABL evolution along the arrow pointing to the east in Fig. 4, and updraft and downdraft areas cross the lidar site from east to west. The arrangement and relative sizes of updraft and downdraft areas in this simplified sketch reflect qualitatively the findings presented in Fig. 5 for the cumuli-topped case (5 April). As illustrated in Fig. 4 updraft cross sections are smaller than downdraft areas which surround these thermals. Downdraft areas may be regarded as diffuse regions (with no clear boundaries), which may often merge, and which are sometimes interrupted by areas with velocities between 0 to −0.1 m/s (environmental air).

By using Eqs. (1) and (2) we analyzed the time series of the vertical velocity $w$ to identify the updraft and downdraft events at different height levels from 525 m height up

to the ABL top height $z_i$. We analyzed the time series from the beginning of convective activity to the end of the ABL lifetime as well as for the convectively most active period from 12:00–17:00 LT (see Fig. 1).

Figure 5 presents the statistics of updraft and downdraft events observed on 5 April. On average, 15 updrafts and 20 downdrafts per hour are counted over the entire day. At cloud level (975 m height level, cloud formation occurred here before 13:30 LT) the updraft occurrence frequency is significantly increased and exceeds the value of the downdraft frequency. Cloud occurrence reinforces the convective activity as a result of latent heat release and horizontally and vertically inhomogeneous radiative heating and cooling. The downdraft occurrence frequency, in turn, is enhanced at 1200 m height. This is probably caused by enhanced entrainment of free tropospheric air into the ABL before 13:30 LT triggered by cloud formation. After 13:30 LT, both the 975 m and the 1200 m height levels are below cloud base.

By keeping the mean wind speed of 4.2 m/s into account, the observed temporal occurrence frequencies correspond to a spatial occurrence frequency of around 1.0 $km^{-1}$ or roughly 1.5 per unit length $z_i$. 50% and 30% of the time series (09:49–16:45 LT) is covered by downward and upward motions, respectively, for almost all analyzed height levels, except for 975 m (45% downward motion, 40% upward motion). In 15%–30% of the time the observations are undefined and indicate environmental air according to Eqs. (1) and (2), i.e., velocities are $-0.1\,m/s > w < +0.1\,m/s$ or the period with negative or positive vertical velocity is <20 s. The mean occurrence duration of the counted updrafts is 50–70 s, which corresponds to a mean horizontal extent of 200–300 m for horizontal wind speeds around 4 m/s. Downdrafts occur, on average, for about 70–100 s which translates to 300–400 m in horizontal extent on that day.

Figures 6 and 7 show the updraft and downdraft characteristics for the other two cases. On 5 May 2006, strong convective motions and a textbook-like development of a cloud-free boundary layer is observed (see Fig. 1). Updraft and downdraft occurrence frequencies are in the range of 16–21 $h^{-1}$ and 22–32 $h^{-1}$, respectively. On this clear day, in about 50% and only 18%–27% of the time downdrafts and updrafts occur,



ACPD
10, 9219–9252, 2010



respectively. About 20%–30% of the time is covered with weak upward and downdraft motions (environmental air).

Schumann and Moeng (1991) performed simulations for a cloud-free boundary layer and horizontal wind speeds of 10 m/s (similar to the conditions on 5 May 2006). Turbulence was mainly driven by buoyancy with small contributions from shear. $w_*$ and $z_i$ were 2.0 m/s and 1030 m in their modelling effort, respectively. As a main result, the area fraction of updrafts was 40%–45% and 50%–55% for the downdrafts in the mixing layer ($z/z_i$ from 0.3–0.7). They counted all areas with positive and negative vertical velocity as updrafts and downdrafts, respectively. The ratio of the simulated downdraft to updraft mean diameter was 1.4–1.5 in the mixed layer from 0.3–0.7 in terms of $z/z_i$ and thus in good agreement with our observations. This ratio mostly ranges from 1.2–1.5 in the central part of the convective ABL on 5 April and 5 May. The simulated frequency of occurrence was of the order of 1–1.5 per unit length $z_i$ in the mixed layer ($z/z_i$ from 0.3–0.7) and thus in the same range of values as observed on 5 April and 5 May 2006.

The much larger mean horizontal extent of the drafts on 5 May (500–600 m updraft mean, 600–900 m downdraft mean extent) compared to the values for 5 April and for 18 September shown in Fig. 7 is related to the fact that only currents that last for longer than 20 s are counted and thus considered in the statistics. At high horizontal wind speeds around 10.5 m/s only drafts with horizontal extents >210 m (cutoff size) are counted, whereas on 5 April (4.2 m/s) and 18 September (1.8 m/s) the cutoff size is 84 m and 36 m, respectively, and consequently the average values of the updraft and downdraft sizes are much lower on 5 April and even lower on 18 September (100–250 m).

The ratio of downdraft to updraft fractional coverage is much higher on the cloud-free 5 May than on the 5 April. The same roughly holds for the downdraft-to-updraft duration ratio or horizontal extent ratio. This behavior is caused by the occurrence of many long lasting updrafts below the cloud bases on 5 April. On the other hand, the downdraft characteristics remains almost unaffected by cloud formation and is thus similar on 5 April and 5 May.

On 18 September 2006, the ABL evolution is complicated by the presence of a lofted dust layer (see Fig. 1). Strong upward and downward motion occur from 13:00–16:30 LT. After 16:15 LT waves appear in the aerosol layer above 1500 m. An airmass change obviously occurs around 16:15 LT.

The updraft and downdraft characteristics on 18 September do not show such a vertically coherent behavior as observed on 5 May 2006. The surface-heating-driven development of updrafts is significantly suppressed on that day. The wave activity observed later at higher altitudes is indicative for comparably stable conditions which may explain the rather low number of updrafts. Downdrafts are a factor of 3 more frequent around 1200 m height than updrafts in Figure 7. The increasing number of updrafts with maximum around 1500–1800 m is related to the systematic up and downward motions associated with the wave activity above 1500 m height after 16:00 LT.

Because of the rather low horizontal wind speed, smaller updrafts and downdrafts with 35–40 m horizontal extent are counted and considered in the statistics as, for example, in the statistics for 5 May. This contrasting feature (low versus high horizontal wind speed) is used in the comparison of the updrat and downdraft characteristics of the three cases which are summarized in Table 1.

To better compare the findings we consider only the central time period of the ABL evolution from 12:00–17:00 LT (until 16:45 LT on 5 April) and the height levels of 525, 750, and 1050 m (see Fig. 1) which are at least on 5 April and 5 May always fully in the ABL. In contrast, on 18 September, the ABL top reaches the 750 and 1050 m height level not before 13:15 and 13:45 LT, respectively. Therefore, we consider only the data sets for the lowest level of 525 m in Table 1 for this day.

During almost 1.5 h (30%–34%) and more than 2.5 hours (52%–57%) of the 5 h period updrafts and downdrafts lasting for longer than 20 s and showing vertical velocities $< -0.1$ m/s or $>0.1$ m/s are observed in the fully developed convective boundary layer disregarding the occurrence of fair weather cumuli, the strength of horizontal wind speed, and ABL height $z_i$. The mean frequency of occurrence of significant updrafts is also remarkably equal at all three days with values of 1.2–1.7 per unit length $z_i$ during

the central time period from 12:00–17:00 LT.

The strong differences in the observed mean horizontal extent and mean vertical velocity values for the three days is caused by the selected 20 s threshold value in the conditional sampling method. As mentioned, the minimum horizontal extent of counted updrafts and downdrafts is 36 m (18 September), 84 m (5 April), and 210 m (5 May). To eliminate this cutoff effect, we assume that on 18 September, the day with lowest horizontal wind speed of 1.8 m/s, all relevant updrafts and downdrafts are counted, and that the frequency distributions of updraft and downdraft sizes found on 18 September holds for the other two days, too. The frequency distribution of updrafts and downdrafts for all three days are presented in Fig. 8. All distributions show an exponential decrease of the relative occurrence frequency of drafts with draft size. Keeping this observed exponential decrease into consideration, 25%–30% of the updrafts and downdrafts, i.e., all drafts with sizes from 36–84 m, remained undetected on 5 April. For the 5 May, we yield that 45%–50% of the downdrafts (drafts with horizontal extents from 36–210 m) remained undetected. If we consider these missing drafts in the statistics, the mean horizontal extent is about 235 m (5 April) and 420 m (5 May) for the updrafts, and 300 m (5 April) and 570 m (5 May) for the downdrafts. These values (estimates for an assumed minimum draft extent of 36 m) are included in Table 1.

As shown in Figs. 9 and 10, larger updrafts and downdrafts show larger vertical velocities, so that also the mean values of draft vertical velocity increase with increasing observational cutoff size. Mean vertical velocities are 0.66 m/s and −0.58 m/s (5 April) and 0.71 and −0.71 m/s (5 May) for updrafts and downdrafts, respectively, when the missing updrafts and downdrafts with sizes down to 36 m are taken into account. If we finally express the corrected values as functions of the boundary layer height $z_i$ and the convective velocity scale $w_*$ given in the table, we end up with values of 0.16–0.18$z_i$ for mean updraft size for all three days, and for the mean updraft velocity with values of 0.4–0.45$w_*$ for all three days disregarding the occurrence of cumulus clouds.

The values are in good agreement with observations of Lenschow and Stephens (1980). They used humidity fluctuations (exceeding a certain threshold value for hor-




izontal extents ≥25 m) over an oceanic site to identify updrafts and downdrafts and found values from $0.08z_i$–$0.15z_i$ for the updraft mean size in the height range from $z/z_i$=0.2 to 0.8. They obtained values of $0.4\pm0.1w_*$ as a mean vertical velocity in updrafts.

Young (1988b) analyzed low-pass filtered vertical velocity time series measured during 58 flight legs, each approximately 35 km long and evenly distributed from height level $0.1z_i$ to $1.3z_i$, and counted any event larger than 40 m in size showing positive vertical velocity as updraft, and the residual data segments (periods) as downdrafts. The observations were performed in the framework of the September 1978 Phoenix Convective Boundary Layer Experiment at the Boulder Atmospheric Observatory. The arithmetic mean updraft width for the individual flight legs ranged from $0.15z_i$ to $0.35z_i$. The arithmetic mean value of the updraft mean vertical velocity was $0.3w_*$–$0.7w_*$ for the range $z/z_i$ from 0.3–0.7. For downdrafts the respective vertical velocities accumulated between $-0.3w_*$ and $-0.6w_*$.

### 3.3 Draft mean velocity versus draft size

To further investigate differences between the evolution of the cloud-free and cloud-topped mixing layer, the dependence of the draft vertical velocity on the size of the updrafts and downdrafts is illuminated. The potential impact of fair weather cumuli on this relationship is presented in Figs. 9 and 10. The mean velocity shown in the figures describe the mean value of all updraft and downdraft vertical velocities found for a given size class (horizontal extent interval). The individual values of updraft or downdraft vertical velocity in this averaging are mean values averaged over the horizontal cross section of the drafts.

We concentrate on the almost textbook-like convective days (5 April, 5 May). All updraft and downdraft events measured at the height levels of 525, 750 and 1050 m during the 12:00–16:45 LT (5 April) and 12:00–17:00 LT time period (5 May) are considered in Fig. 9. A clear tendency is observed. On average, the updraft mean velocity increases from about 0.5 m/s for small drafts (small with respect to their horizontal ex-





tent) to 1.5 m/s for large thermals with horizontal extents of 600–1000 m (150–250 s duration interval in Fig. 9). The mean updraft velocities are at all larger for the different size classes on 5 April, most probably a result of cloud convection. The velocity-versus-size characteristics for downdrafts is very similar on the two days. Maximum downdraft velocities accumulate from 0.8–1.2 m/s for large drafts on both days.

In Fig. 10, the influence of the boundary depth $z_i$ on the relationship between velocity and size is removed by dividing the draft width $d$ by $z_i$. $d$ and $z_i$ were measured simultaneously with Doppler lidar and small aerosol lidar, respectively. Furthermore the velocities are normalized by using the convective velocity scale $w_*$. The time series of $w_*$ obtained from 1-h and 2-h $\sigma_w^2(z)$ profiles as shown in Fig. 2 did not show any trend over the day so that we simply used $w_*$ from Table 1 for this normalization.

The dependence of the normalized downdraft mean velocity on $d/z_i$ is almost the same on 5 April and 5 May for normalized downdraft sizes <0.6, but then decreases with draft size on the day with cloud development (5 April). The curves describing the dependence of the updraft mean vertical velocity on draft size show a steeper slope than the respective downdraft curves. The strongest velocity increase with increasing updraft extent is found on 5 April caused by cloud convection. Even if we take the atmospheric variability into account, the mean values are at all larger on 5 April than on 5 May and clearly show the cloud impact. The vertical velocity is, on average, about 20% stronger in the large thermals on the day with cloud convection.

Figure 11 corroborates the hypothesis that the formation of fair weather cumuli is the reason for the development of stronger updrafts showing higher velocities. Two periods already shown in Fig. 1 are presented. Vigorous updrafts with occurrence lengths of 180–220 s, which corresponds to horizontal extents of 800–1000 m, and thermal mean velocities of up to 1.5–3 m/s are visible below the clouds. In the cores of these updrafts vertical winds are sometimes about a factor of two higher than the plume mean vertical velocity. These clouds already develop during the morning hours when the boundary layer height is about 1000 m. In the afternoon, cloud base height is 500 m higher, boundary layer height is close to 1600–1700 m, and the updrafts below the cloud base

are still pronounced (occurrence duration frequently > 100 s) but less intense (updraft mean velocities from 1–2 m/s).

Kollias et al. (2001) analyzed radar observations of the updraft and downdraft behavior in fair weather cumuli and stated that even small cumuli with horizontal extents of the order of 1000 m (as the smaller ones in Fig. 11) should be considered as convective complexes rather than simple growing elements that later decay into passive clouds. The two cumuli studied by Kollias et al. (2001) consisted of an updraft core of 400 m width surrounded by narrow downdrafts (100 m width). In these clouds with a vertical depth of about 700 m updraft velocities of about 5.5 m/s were observed. The updraft core structure suggested that the cumulus clouds were composed of successive bubbles that emerge from the subcloud layer. Figure 11 (afternoon period) is in accordance with this explanation. The interaction of the turbulent mixing processes in ABL and the evolution of convective clouds in the upper part of the ABL are closely coupled. Large thermals initiate the development of cumuli and, in the subsequent step, the freshly formed clouds reinforce the thermals (chimney effect) and may combine smaller updrafts to larger ones, which in turn is of advantage to stimulate deeper convection of the developing cloud towers.

## 4 Conclusions

In summary, a first comprehensive Doppler lidar study on the updraft and downdraft characteristics in the boundary layer has been presented. As a new aspect, we contrasted the evolution of the ABL at cloud-free and cloudy conditions. The high quality data sets of vertical wind observations enabled us to analyze the relationship between the horizontal extent of the updraft and downdrafts and their mean vertical velocity.

Three cases of the diurnal evolution of the atmospheric boundary layer over the flat rural/urban Leipzig area, Germany, were studied. The counted updraft events covered 30%–34%, the downdrafts 53%–57% of the velocity time series during the main convective periods around noon and the early afternoon. During the day with fair weather




cumuli, the frequency of occurrence of downdrafts and updrafts was enhanced by a factor of about 1.5 at cloud height level and at height levels close to cloud base. The mean horizontal extent of the updrafts ranged from 200–420 m and from 0.16–0.18 in terms of the ratio of updraft width to boundary layer depth when all coherent features with horizontal extents of >36 m were considered in the statistics. Downdrafts were found to be, on average, a factor of 1.3–1.5 larger than updrafts regarding the horizontal extent. The average value of the updraft vertical velocities ranged from 0.5–0.7 m/s. The ratio of the updraft mean velocity to the convective velocity scale was about 0.4–0.45 at all three days disregarding the occurrence of clouds. All these values agreed well with the literature and indicated the high quality of our Doppler lidar observations.

The relationship between the horizontal extent of the updrafts and downdrafts and their mean vertical velocity was highlighted. This analysis revealed a pronounced increase of the average vertical velocity of the updrafts from values around 0.4–0.5 m/s for small thermals (100–200 m, $d/z_i$ of 0.1–0.15) to about 1.5 m/s for large thermals (>600 m, $d/z_i$ from 0.6–0.8) in the case with fair weather cumuli.

As an outlook, more contrasting (cloudy versus cloud-free) studies are necessary to corroborate our findings. Especially more cases with cumulus congestus, i.e., clouds which are able to deeply penetrate into the free troposphere, must be monitored and analyzed. Meanwhile, several campaigns have been conducted with our Doppler lidar. Besides the half-year AVEC 2006 campaign, we performed intensive field observations in the tropics (Cape Verde in 2008) and in southwestern Germany in orographically complex terrain in the summer of 2007. Future Doppler and aerosol/cloud/polarization lidar studies at Leipzig will focus on fair-weather cloud-topped boundary layers, aerosol-cloud interactions, and the role of turbulence in this context.





## References


Ansmann, A., Tesche, M., Knippertz, P., Bierwirth, E., Althausen, D., Müller, D., and Schulz, O.: Vertical profiling of convective dust plumes in southern Morocco during SAMUM, Tellus B, 61, 340–353, 2009. 9221

Baars, H., Ansmann, A., Engelmann, R., and Althausen, D.: Continuous monitoring of the boundary-layer top with lidar, Atmos. Chem. Phys., 8, 7281–7296, 2008, http://www.atmos-chem-phys.net/8/7281/2008/. 9223

Bösenberg, J. and Linné, H.: Laser remote sensing of the planetary boundary layer, Meteorol. Z., 11, 233–240, 2002. 9222

Drobinski, P., Carlotti, P., Newsom, R. K., Banta, R. M., Foster, R. C., and Redelsperger, J.-L.: The structure of the near-neutral atmospheric surface layer, J. Atmos. Sci., 61, 699–714, 2004. 9222

Durand, P., Thoumieux, F., and Lambert, D.: Turbulent length–scales in the marine atmospheric mixed layer, Q. J. Roy. Meteorol. Soc., 126, 1889–1912, 2000. 9222

Engelmann, R.: Aerosol vertical exchange in the convective planetary boundary layer, Dissertation, University of Leipzig, 2009. 9223

Engelmann, R., Wandinger, U., Ansmann, A., Müller, D., Zeromskis, E., Althausen, D., and Wehner, B.: Lidar observations of the vertical aerosol flux in the planetary boundary layer, J. Atmos. Ocean. Tech., 25, 1296–1306, 2008. 9222, 9223

Fruntke, J.: Charaktersierung der Grenzschicht anhand von Vertikalwindmessungen mit einem Doppler–Lidar, (Characterization of the boundary layer by means of vertical wind measurements with Doppler lidar), Diploma thesis, University of Leipzig, 2009. 9223

Gibert, F., Cuesta, J., Yano, J.-I., Arnault, N., and Flamant, P. H.: On the correlation between convective plume updrafts and downdrafts, lidar reflectivity and depolarization ratio, Bound.-Lay. Meteorol., 125, 553–573, 2007. 9222

Godowitch, J. M.: Characteristics of vertical turbulent velocities in the urban convective boundary layer, Bound.-Lay. Meteorol., 35, 387–407, 1986. 9222

Greenhut, G. K. and Khalsa, S. J. S.: Updraft and downdraft events in the atmospheric boundary layer over the equatorial Pacific Ocean, J. Atmos. Sci., 39, 1803–1817, 1982. 9221, 9222, 9224

Greenhut, G. K. and Khalsa, S. J. S.: Convective elements in the marine atmospheric boundary layer. Part I: conditional sampling studies, J. Clim. Appl. Meteorol., 26, 813–822, 1987. 9221,






9224
Grund, C. J., Banta, R. M., George, J. L., Howell, J. N., Post, M. J., Richter, R. A., and Weickmann, A. M.: High-resolution Doppler lidar for boundary layer and cloud research, J. Atmos. Ocean. Tech., 18, 376–393, 2001. 9222
Hogan, R. J., Grant, A. L. M., Illingworth, A. J., Pearson, G. N., and O'Connor, E. J.: Vertical velocity variance and skewness in clear and cloud-topped boundary layers as revealed by Doppler lidar, Q. J. Roy. Meteorol. Soc., 135, 635–643, 2009. 9222, 9227
Khalsa, S. J. S. and Greenhut, G. K.: Conditional sampling of updrafts and downdrafts in the marine atmospheric boundary layer, J. Atmos. Sci., 42, 2550–2562, 1985. 9221, 9222
Kollias, P., Albrecht, B. A., Lhermitte, R., and Savtchenko, A.: Radar observations of updrafts, downdrafts, and turbulence in fair-weather cumuli, J. Atmos. Sci., 58, 1750–1766, 2001. 9221, 9234
Lenschow, D. H.: Airplane measurements of planetary boundary layer structure, J. Appl. Meteorol., 9, 874–884, 1970. 9221
Lenschow, D. H. and Stephens, P. L.: The role of thermals in the convective boundary layer, Bound.-Lay. Meteorol., 19, 509–532, 1980. 9221, 9222, 9231
Lenschow, D. H. and Stephens, P. L.: Mean vertical velocity and turbulence intensity inside and outside thermals, Atmos. Environ., 16, 61–64, 1982. 9225
Lenschow, D. H., Mann, J., and Kristensen, L.: How long is long enough when measuring fluxes and other turbulence statistics?, J. Atmos. Ocean. Tech., 11, 661–673, 1994. 9243
Lothon, M., Lenschow, D. H., and Mayor, S. D.: Coherence and scale of vertical velocity in the convective boundary layer from Doppler lidar, Bound.-Lay. Meteorol., 35, 387–407, 1986. 9222
Moeng, C.-H. and Rotunno, R.: Vertical–velocity skewness in the buoyancy–driven boundary layer, J. Atmos. Sci., 47, 1149–1162, 1990. 9227
Said, F., Canut, G., Durand, P., Lohou, F., and Lothon, M.: Seasonal evolution of boundary–layer turbulence measured by aircraft during the AMMA 2006 Special Observation Period, Q. J. Roy. Meteorol. Soc., 135, 47–65 , 2010. 9222
Schumann, U. and Moeng, C.-H.: Plume fluxes in clear and cloudy convective boundary layers, J. Atmos. Sci., 48, 1746–1757, 1991. 9229
Seifert, P., Engelmann, R., Ansmann, A., Wandinger, U., Mattis, I., Althausen, D., and Fruntke, J.: Characterization of specular reflections in mixed–phase and ice clouds based on scanning, polarization, and Raman lidar, in: Reviewed and revised papers presented at the 24th





International Laser Radar Conference, 23–28 June 2008, Boulder, Colorado, USA, edited by: Hardesty, M. and Mayor, S., 571–574, NOAA, Boulder, Co, ISBN 978-0-615-21489-4, 2008. 9223

Stull, R. B.: An Introduction to Boundary Layer Meteorology, Kluwer Academic Publishers, Dordrecht, 666 pp., 1988. 9224, 9225, 9227

Williams, A. G. and Hacker, J. M.: The composite shape and structure of coherent eddies in the convective boundary layer, Bound.-Lay. Meteorol., 61, 213–245, 1992. 9222, 9224

Wulfmeyer, V. and Janjić, T.: Twenty-four-hour observations of the marine boundary layer using shipborne NOAA high-resoultion Doppler lidar, J. Appl. Meteorol., 44, 1723–1744, 2005. 9222

Young, G. S.: Turbulence structure of the convective boundary layer. Part I: variability of normalized turbulence statistics, J. Atmos. Sci., 45, 719–726, 1988a. 9221

Young, G. S.: Turbulence structure of the convective boundary layer. Part II: Phoenix 78 aircraft observations of thermals and their environment, J. Atmos. Sci., 45, 727–735, 1988b. 9221, 9222, 9224, 9232

Young, G. S.: Convection in the atmospheric boundary layer, Earth-Sci. Rev., 25, 179–198, 1988c. 9221





**Table 1.** Summary of updraft and downdraft properties for the three cases discussed. Mean values (and partly standard deviations) are presented for the time period from 12:00–17:00 LT on 5 May and 18 September and from 12:00–16:45 LT on 5 April, and by considering the vertical velocity times series for the height levels of 525, 750, and 1050 m on 5 April and 5 May. Occurrence parameters for the 18 September are computed from the data sampled at the 525 m height level only. The integrated occurrence time (fractional coverage in percent) is related to the total 4.75 h and 5 h observation periods, occurrence rate is calculated from the number of detected drafts during the total period of 4.75–5 h. Mean horizontal extent is simply obtained by the mean draft occurrence period (in seconds) multiplied by the estimated wind speed given in the table. Minimum horizontal size (cutoff size) of counted drafts is indicated in the table (84 m, 210 m, 36 m). Estimates of draft mean size and velocity for a cutoff size of 36 m are given in addition.

| | 5 April 2006 | 5 May 2006 | 18 September 2006 |
|---|---|---|---|
| Clouds | Fair weather cumuli | Cloud-free | Few cumuli |
| Wind speed ($z$=0.5–1 km, estimate) | 4.2 m/s | 10.5 m/s | 1.8 m/s |
| Boundary layer height $z_i$ | 1.45 km | 2.3 km | 1.3 km |
| Convective velocity scale $w_*$ | 1.5 m/s | 1.75 m/s | 1.3 m/s |
| Updrafts (cutoff size) | 84 m | 210 m | 36 m |
| Occurrence (fractional coverage) | 34% | 31% | 30% |
| Occurrence rate | 0.30 $min^{-1}$ | 0.32 $min^{-1}$ | 0.14 $min^{-1}$ |
| Occurrence frequency | 1.2 $km^{-1}$ | 0.5 $km^{-1}$ | 1.3 $km^{-1}$ |
| Occurrence frequency | 1.7 $z_i^{-1}$ | 1.2 $z_i^{-1}$ | 1.7 $z_i^{-1}$ |
| Mean horizontal extent $d_{up}$ | 289±314 m | 622±725 m | 203±278 m |
| Mean vertical velocity $w_{up}$ | 0.76±0.59 m/s | 0.91±0.71 m/s | 0.55±0.51 m/s |
| $d_{up}$ (cutoff size = 36 m) | 235 m | 417 m | 203 m |
| $d_{up}$ (cutoff size = 36 m) | 0.16 $z_i^{-1}$ | 0.18 $z_i^{-1}$ | 0.16 $z_i^{-1}$ |
| $w_{up}$ (cutoff size = 36 m) | 0.66 m/s | 0.71 m/s | 0.55 m/s |
| $w_{up}$ (cutoff size = 36 m) | 0.44 $w_*$ | 0.41 $w_*$ | 0.42 $w_*$ |
| Downdrafts (cutoff size) | 84 m | 210 m | 36 m |
| Occurrence (fractional coverage) | 53% | 54% | 57% |
| Occurrence rate | 0.35 $min^{-1}$ | 0.40 $min^{-1}$ | 0.23 $min^{-1}$ |
| Mean horizontal extent $d_{do}$ | 374±329 m | 848±890 m | 295±492 m |
| Mean vertical velocity $w_{do}$ | −0.65±0.49 m/s | −0.89±0.72 m/s | −0.43±0.35 m/s |
| $d_{do}$ (cutoff size = 36 m) | 304 m | 569 m | 295 m |
| $w_{do}$ (cutoff size = 36 m) | −0.58 m/s | −0.71 m/s | −0.43 m/s |



ACPD
10, 9219–9252, 2010



**Table 2.** Fit parameters (± standard deviation) describing the exponential curves in Fig. 8. The function is $N_d = A\exp(-d/B)$ with the number of updrafts or downdrafts $N_d$ and horizontal extent $d$.

| | A | B |
|---|---|---|
| Updrafts, downdrafts, 5 May | 61.24±4.54 | 318.42±17.43 |
| Updrafts, downdrafts, 18 Sep | 28.04±2.36 | 78.15±6.08 |
| Updrafts, downdrafts, 5 Apr | 38.34±1.93 | 164.14±7.29 |





**Table 3.** Fit parameters (standard deviation in brackets) describing the line curves in Fig. 10. The function is $\overline{w_D}/w_* = A + B1(d/z_i) + B2(d/z_i)^2$. For downdrafts, $\overline{w_D}/w_*$ must be multiplied by −1.

| | A | B1 | B2 |
|---|---|---|---|
| Updrafts, 5 Apr | 0.30±0.053 | 1.27±0.28 | −0.43±0.31 |
| Updrafts, 5 May | 0.30±0.041 | 1.02±0.22 | −0.45±0.24 |
| Downdraft, 5 Apr | 0.20±0.028 | 1.49±0.15 | −1.31±0.16 |
| Downdraft, 5 May | 0.29±0.024 | 0.94±0.13 | −0.54±0.14 |





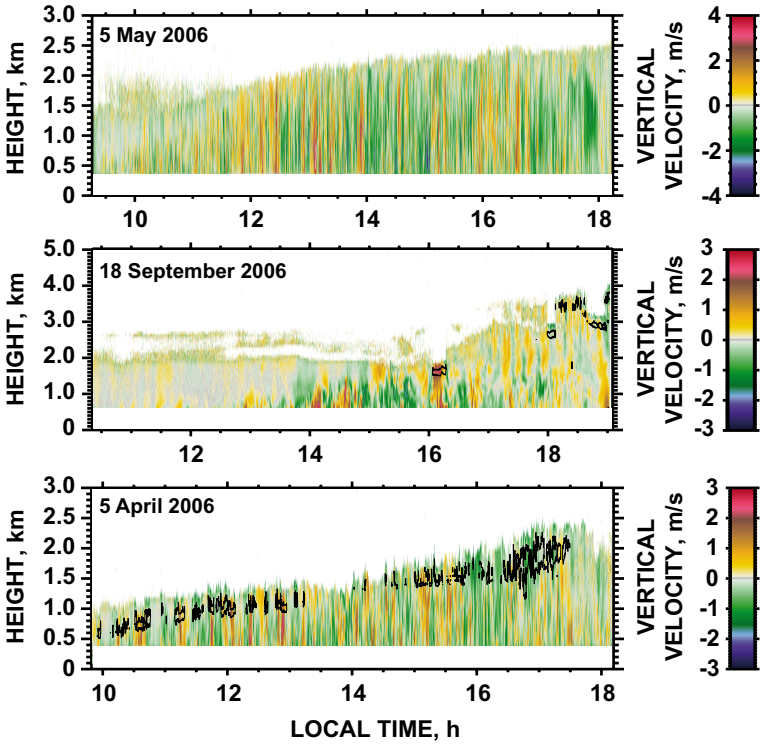


**Fig. 1.** Evolution of the ABL in terms of vertical velocity observed with Doppler lidar (resolution: 5 s, 75 m) at Leipzig on 5 May 2006 (top), 18 September 2006 (center), and 5 April 2006 (bottom). Yellow and red (positive velocities) indicate upward movements, whereas green and blue (negative velocities) represent downward movements. The top of the area with colored velocity values approximately coincides with the ABL top height. Convective clouds are indicated by black contour lines. Lidar signals from the near range (region of detector saturation) are not trustworthy and thus not shown. 12:00 Local Time (LT, daylight saving time) is 11:00 Central European Time (CET) and 10:00 UTC.



ACPD
10, 9219–9252, 2010



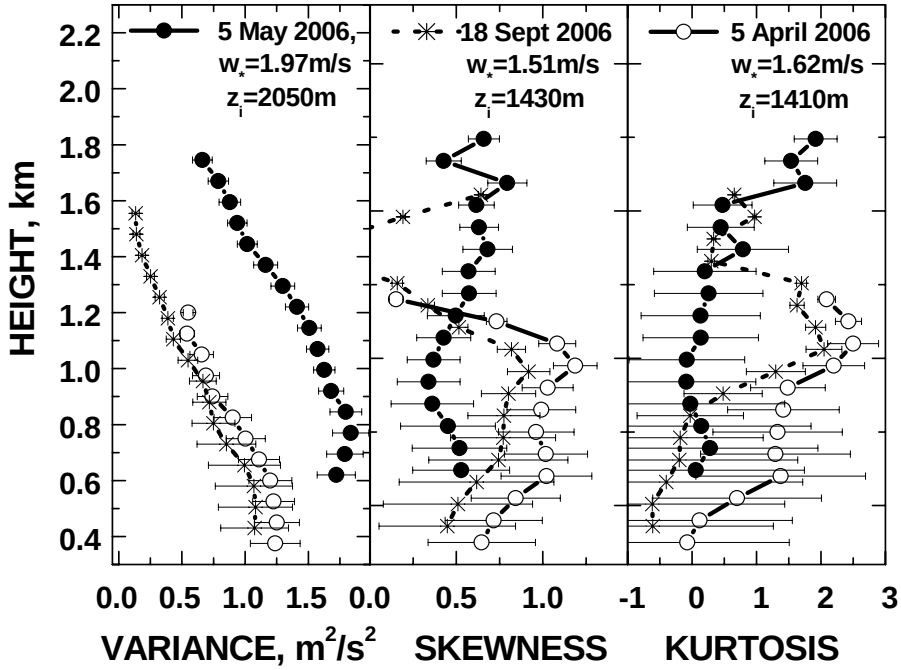


**Fig. 2.** Variance, skewness, and kurtosis of vertical velocity considering measurements from 12:00–14:00 LT on 5 April and 5 May 2006, and from 14:00–16:00 LT on 18 September 2006. Error bars indicate sampling errors calculated after Lenschow et al. (1994). Instrumental noise is very low. Values for the convective scale $w_*$ and mixing-layer top height $z_i$ for the analyzed two-hour periods are given as numbers.

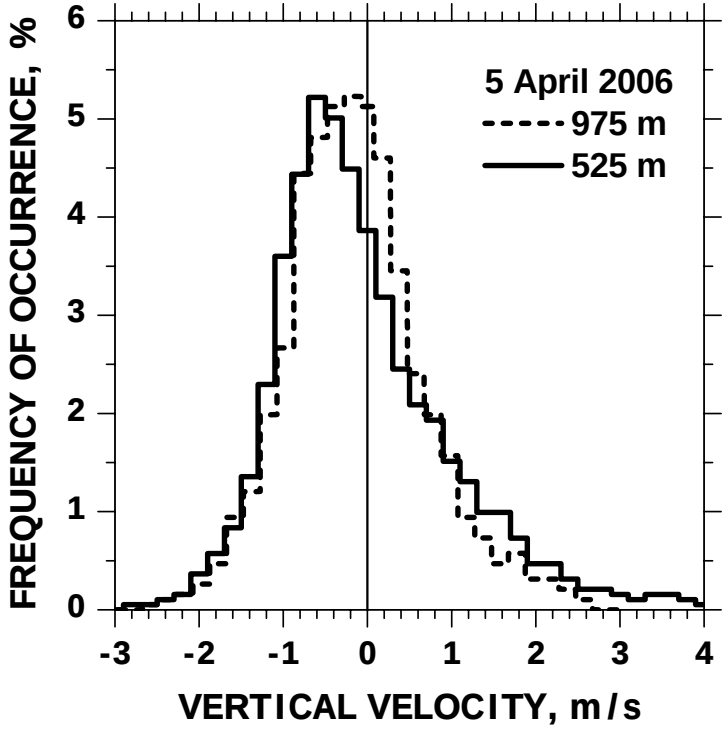


**Fig. 3.** Frequency of occurrence of vertical velocity measured with Doppler lidar on 5 April from 09:49–16:45 LT. Distributions are presented for 525 m height (lower ABL) and 975 m height (upper ABL before 14:00 LT).



ACPD
10, 9219–9252, 2010



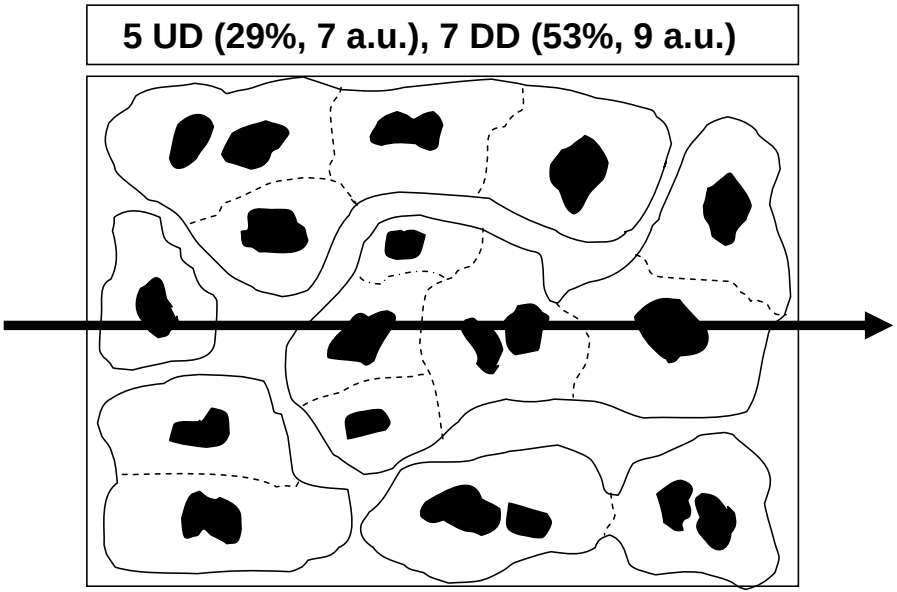


**Fig. 4.** Top view on the convectively active PBL. The idealized scenario is in qualitative agreement with Fig. 5. Well-defined small areas of updrafts (UD, black) are surrounded by zones with downward motion (DD, white). The DD zones partly merge (indicated by dashed lines). The thick horizontal vector, pointing to the east, illustrates what a Doppler lidar observes in case of easterly winds regarding draft frequency (5 UD, 7 DD zones), occurrence duration or horizontal extent (updraft mean extent of 7 arbitrary units, a.u., downdraft mean extent of 9 a.u.), and how much of the area is covered by updrafts (29%) and by downdraft zones (53%). The remaining area (18%) is covered by environmental air ($-0.1\,\mathrm{m/s} > w < 0.1\,\mathrm{m/s}$).

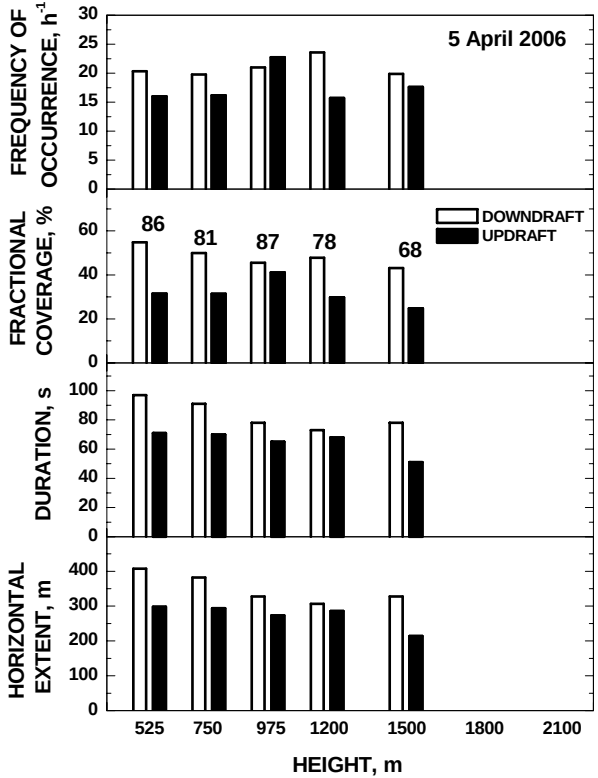


**Fig. 5.** Mean frequency of occurrence, fractional coverage of up and downdrafts (defined by Eq. 1 and Eq. 2), mean occurrence duration of the up- and downdrafts, and corresponding mean horizontal extent according to mean horizontal wind speed of 4.2 m/s as estimated from nearby radiosonde information and atmospheric modeling. Statistics are separately shown for updrafts (black columns) and downdrafts (white columns) for heights of 525, 750, 975, 1200, and 1500 m and for time periods during which vertical velocities could continuously be measured within the entire observational period from 09:49 and 16:45 LT (07:49–14:45 UTC) on 5 April 2006. The total temporal coverage with both updrafts and downdrafts is given as number (in %) for the different investigated height levels (see fractional coverage plot). About 15%–30% of the time environmental air prevailed, i.e, the draft periods were <20 s and/or $-0.1\,\text{m/s} > w < +0.1\,\text{m/s}$.

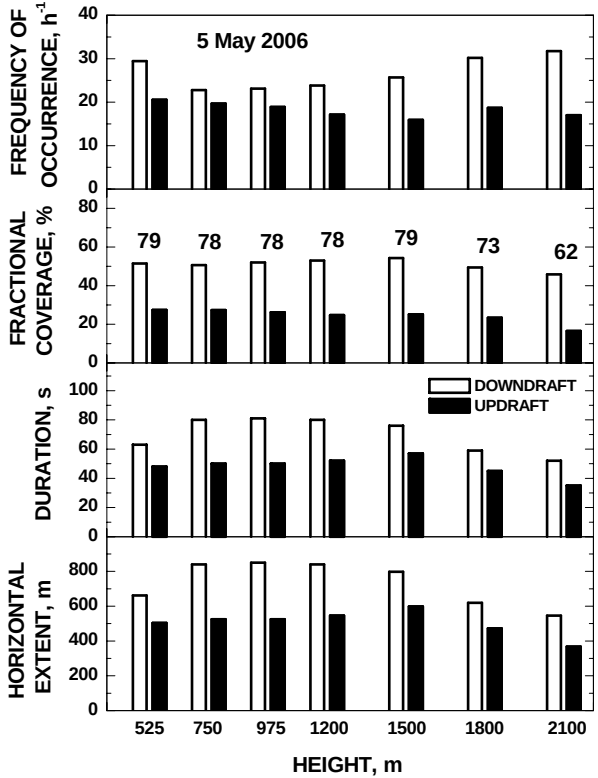


**Fig. 6.** Same as Fig. 5, except for 5 May 2006, 09:15–18:14 LT (07:15–16:14 UTC).

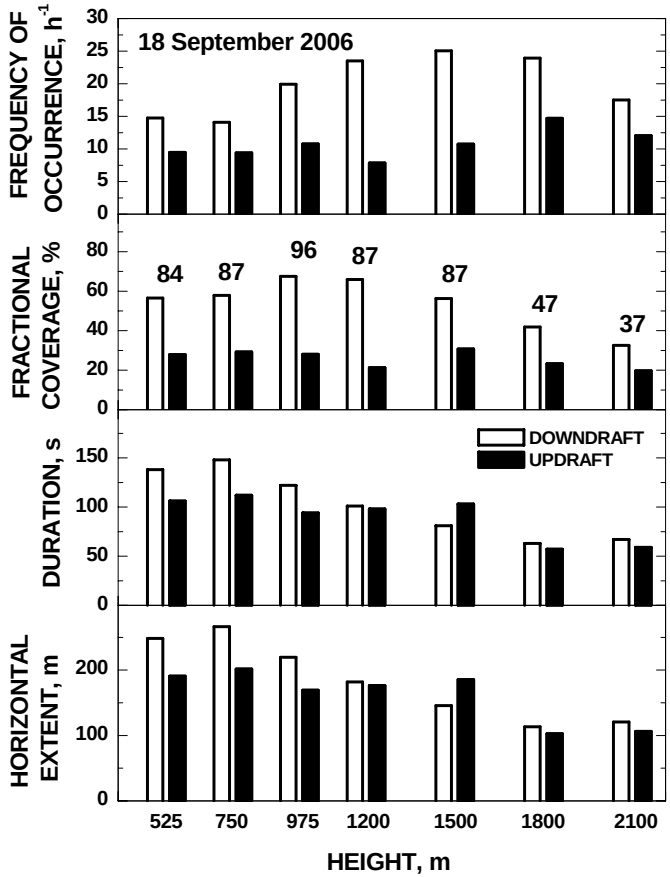


**Fig. 7.** Same as Fig. 5, except for 18 September 2006, 1020–1905 (08:20–17:05 UTC).

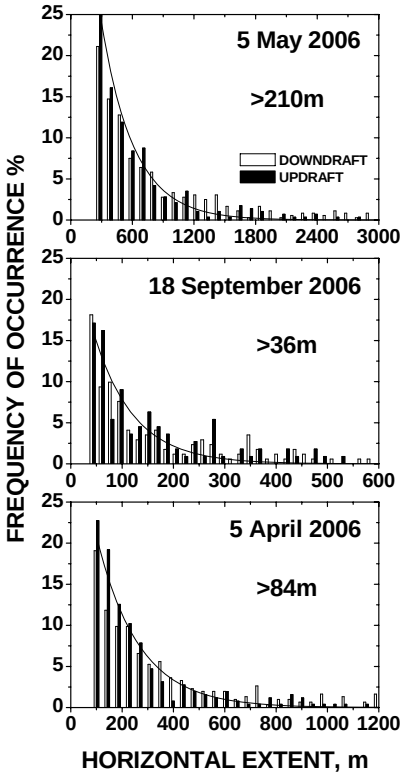


**Fig. 8.** Frequency of occurrence of updraft (black) and downdraft (white) horizontal extents (observed occurrence duration > 20 s times horizontal wind speed) for 10 s occurrence duration intervals (20–30 s, 30–40 s, etc.). The statistical results consider all updraft and downdraft events observed at the 525, 750, and 1050 m height levels on 5 April, 12:00–16:45 LT and on 5 May and 18 September, 12:00–17:00 LT. Curves (exponential functions) are fitted to the observed updrafts and downdrafts. Fit parameters are given in Table 2.

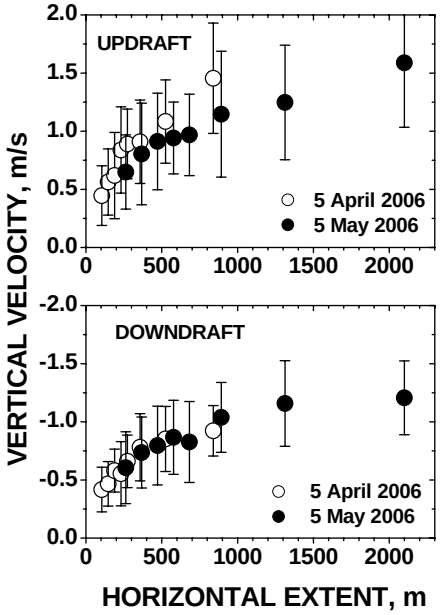


**Fig. 9.** Updraft mean **(a)** and downdraft mean vertical velocities **(b)** as a function of draft horizontal extent (temporal length of the observed updraft and downdraft periods times horizontal wind speed). Average values (symbols) and standard deviations (vertical bars) are presented for eight occurrence duration intervals (20–30 s, 30–40 s, 40–50 s, 50–60 s, 60–70 s, 70–100 s, 100–150 s, and 150–250 s). For each of the four scenarios (5 April and 5 May, updrafts and downdrafts) 30–90 events were available for intervals from 20–30 s 40–50 s, and 20–50 events for the larger occurrence time intervals. The statistical results consider all updraft and downdraft events observed at the 525, 750, and 1050 m height levels on 5 April, 12:00–16:45 LT and on 5 May, 12:00–17:00 LT.

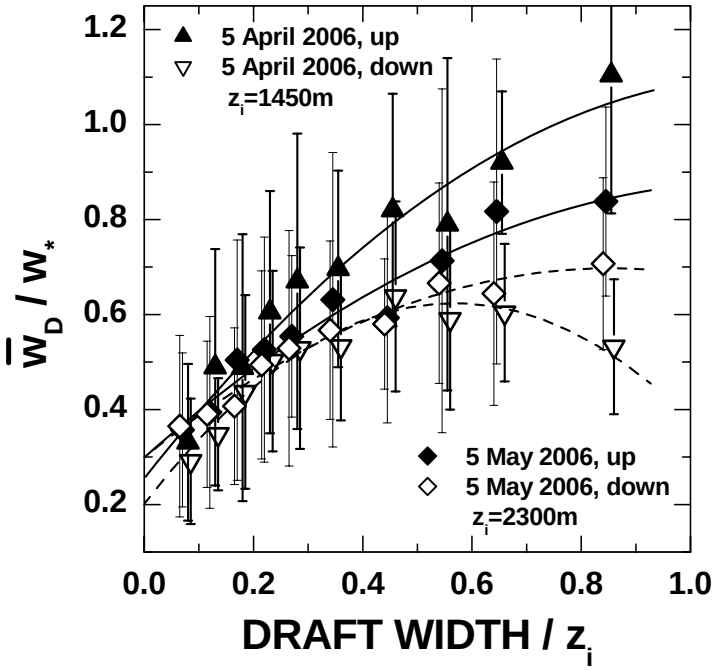


**Fig. 10.** Draft mean vertical velocities $\overline{w_D}$ normalized to the convective velocity scale $w_*$ versus draft width normalized to the ABL top height $z_i$. Curves (polynomial functions) are fitted to the observed data. Fit parameters are given in Table 3.



ACPD
10, 9219–9252, 2010



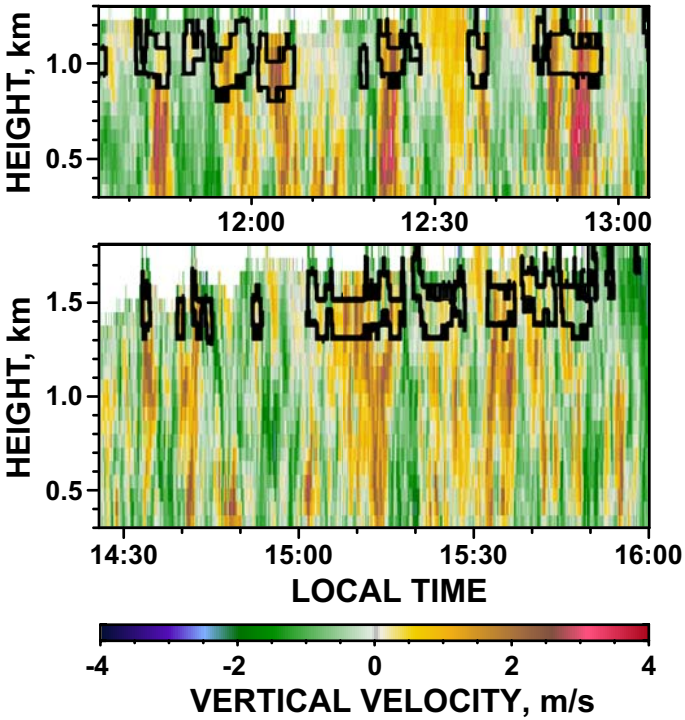


**Fig. 11.** Updrafts below cumulus clouds observed on 5 April 2008, in the early stage of the ABL evolution (top, 11:30–13:00 LT) and close to its end (bottom, 14:30–16:00 LT). The horizontal extent of the strong updrafts around 11:45, 12:22, and 12:53 LT is about 800–1000 m, and the updraft mean velocity ranges from 1.6–2.4 m/s. Peak velocity values in the updrafts frequently exceed 3 m/s, sometimes 4 m/s. In the afternoon less coherent updraft structures are observed below the clouds.



ACPD
10, 9219–9252, 2010